

Microstructure and temperature dependence of properties of morphotropic phase boundary $\text{Bi}(\text{Mg}_{1/2}\text{Ti}_{1/2})\text{O}_3\text{-PbTiO}_3$ piezoceramics processed by conventional routes

Alberto Moure^{a,*}, Miguel Alguero^a, Lorena Pardo^a, Erling Ringgaard^b, Annette F. Pedersen^b

^a Instituto de Ciencia de Materiales de Madrid, CSIC. Cantoblanco, 28049 Madrid, Spain

^b Ferroperm Piezoceramics A/S. Hejreskovej 18A, 3490 Kvistgaard, Denmark

Received 25 July 2005; received in revised form 19 October 2005; accepted 23 October 2005

Available online 28 September 2006

Abstract

Ceramics in the $(1-x)\text{Bi}(\text{Mg}_{1/2}\text{Ti}_{1/2})\text{O}_3\text{-(}x\text{)PbTiO}_3$ system with $x = 0.38, 0.40$ and 0.42 have been processed by conventional sintering from ceramic powders synthesised by one step, direct solid-state reaction of the constituent oxides at 900°C . Coexistence of rhombohedral and tetragonal phases was observed for the three compositions, in good agreement with the very recent report of a morphotropic phase boundary (MPB) in the system at $x \sim 0.37$. The microstructure was characterised, and dielectric properties as a function of temperature and frequency were studied. Permittivity presented two maxima with temperature at $300\text{--}400^\circ\text{C}$ and $\sim 600^\circ\text{C}$. The dielectric anomalies were observed both on heating and cooling and showed hardly any dispersion. Therefore, they are most probably associated with phase transitions, the one at a higher temperature associated with the ferroelectric to paraelectric phase transition. Ceramics were poled and piezoelectric properties were studied, also as a function of temperature. Poling fields up to 5 kV mm^{-1} could be applied, and room temperature d_{33} values between 100 and 166 pC N^{-1} were achieved, depending on composition and sintering temperature. Depoling was found to occur well below the Curie temperature, between 200 and 300°C , also depending on sintering temperature. This composition system seems promising for electromechanical transduction in the intermediate range of temperatures between 200 and 300°C and has the potential of reaching higher temperatures because of its Curie temperature at $\sim 600^\circ\text{C}$.

© 2005 Elsevier Ltd. All rights reserved.

Keywords: Dielectric properties; Piezoelectric properties; Perovskites; Morphotropic phase boundary; $\text{Bi}(\text{Mg,Ti})\text{O}_3$

1. Introduction

Currently, the most used piezoelectric material for operation at high temperature is quartz (SiO_2), in the form of single crystal.¹ Its advantages are high resistivity and practically temperature independent properties in certain cuts (SC, AT, FC, IT, BT, and RT). However, piezoelectric coefficients are low ($d_{11} = 2.3\text{ pC N}^{-1}$), and the maximum working temperature is limited to 350°C .² As one of the alternatives, ferroelectric ceramic materials with high Curie temperature that maintain a stable piezoelectric activity up to high temperatures are under active research.

Ferro-piezoelectric ceramics are the dominant technology for room temperature (RT) electromechanical transduction. It

is well known that a high piezoelectric activity is achieved in lead zirconate titanate (PZT) ceramics at the morphotropic phase boundary (MPB PZT). This is a composition around which three phases with different distortion of the perovskite structure (rhombohedral, tetragonal and monoclinic) exist. The high piezoelectric activity originates from a mechanism of polarization rotation among the different phases. Values of the piezoelectric coefficient d_{33} of $\sim 400\text{ pC N}^{-1}$ are obtained for MPB PZT.² The most widely used piezoelectric materials are various types of doped PZT, whose piezoelectric activity is further enhanced by compositional modification. Commercial piezoceramics, with highest d_{33} values in the range of $400\text{--}600\text{ pC N}^{-1}$ for soft PZT (donor doping), operate at maximum temperatures of $200\text{--}250^\circ\text{C}$.³ Promising results have been also obtained for single crystals of other systems with MPBs, such as $\text{Pb}(\text{In}_{1/2}\text{Nb}_{1/2})\text{O}_3\text{-PbTiO}_3$ ⁴, with $T_C \sim 260^\circ\text{C}$ (lower than PZT), and $\text{Pb}(\text{Yb}_{1/2}\text{Nb}_{1/2})\text{O}_3\text{-PbTiO}_3$,⁵ with $T_C \sim 350^\circ\text{C}$, but for which piezoelectric activity vanishes at $\sim 170^\circ\text{C}$.⁶

* Corresponding author. Tel.: +34 91 3349000x230; fax: +34 91 3720623.
E-mail address: amoure@icmm.csic.es (A. Moure).

Other lead containing, yet non-MPB, materials with higher T_C have been considered and are used as alternatives. One example is lead titanate, PbTiO_3 ($d_{33} = 56 \text{ pC N}^{-1}$, $T_C = 490^\circ\text{C}$), commercially available with lanthanum, samarium and calcium doping that enhances the piezoelectric properties but reduces its operating temperature.^{2,7–9} Another example is lead metaniobate, PbNb_2O_6 with tungsten-bronze structure. It has acceptable piezoelectric properties ($d_{33} = 85 \text{ pC N}^{-1}$), but still relatively low operating temperature ($T_{\text{max}} \sim 300^\circ\text{C}$).²

There is an increasing demand for materials for operation at higher temperatures ($300\text{--}500^\circ\text{C}$),¹⁰ and bismuth-layered structure ferroelectrics (BLSF) are good candidates because of their very high Curie temperature. These materials have as general formula $(\text{Bi}_2\text{O}_2)(\text{A}_{n-1}\text{B}_n\text{O}_{3n+1})$ and their crystalline structure is built by alternating $[\text{Bi}_2\text{O}_2]^{2+}$ and n pseudo-perovskite layers.^{11,12} The major component of the spontaneous polarization lies in the a – b plane of the perovskite-like layers. Piezoelectric activity at 500°C ($d_{31} = 2.1 \text{ pC N}^{-1}$, $k_p = 2.9\%$) has been recently reported in $(\text{SrBi}_2\text{Nb}_2\text{O}_9)_{0.35}(\text{Bi}_3\text{TiNbO}_9)_{0.65}$ compositions ($T_C = 760^\circ\text{C}$).¹³ Some of these compounds, such as $\text{Na}_{0.5}\text{Bi}_{4.5}\text{Ti}_4\text{O}_{15}$ ($T_C = 600^\circ\text{C}$, $d_{33} = 18 \text{ pC N}^{-1}$ at RT)² and PZ46 from Ferroperm Piezoceramics A/S (maximum use temperature of 550°C),³ are commercially available and are used in accelerometers operating at high temperature. High conductivity that makes poling difficult and limits the performance at the highest temperatures is an issue for a number of bismuth layered structure ceramic materials, mainly when they are highly textured.

Recently, new ferroelectric perovskite morphotropic phase boundary (MPB) materials with the ferroelectric to paraelectric phase transition at temperatures exceeding that of PZT, have started to be investigated.¹⁴ Promising results have been obtained for the system $(1-x)\text{BiScO}_3$ – $x\text{PbTiO}_3$. Ceramics around the MPB at $x = 0.64$ present values of $d_{33} = 460 \text{ pC N}^{-1}$, and have a T_C of 450°C .¹⁵ Ultrahigh piezoelectricity was also found for rhombohedral single crystals with $x = 0.57$, which presented a d_{33} of 1150 pC N^{-1} and a T_C of 402°C . It was also shown¹⁶ that piezoelectric activity was maintained up to 340°C . MPBs in other systems such as $(1-x)\text{Bi}(\text{Ga}_{1/4}\text{Sc}_{3/4})\text{O}_3$ – $x\text{PbTiO}_3$ (with $d_{33}(\text{max}) = 124 \text{ pC N}^{-1}$ and $T_C = 465\text{--}510^\circ\text{C}$)¹⁷ and $(1-x)(\text{Bi},\text{La})(\text{Ga}_{0.05}\text{Fe}_{0.95})\text{O}_3$ – $x\text{PbTiO}_3$ (with $d_{33}(\text{max}) = 295 \text{ pC N}^{-1}$ and $T_C = 264\text{--}386^\circ\text{C}$)¹⁸ have been reported. However, the potential applications of these systems are limited by the high cost of Sc_2O_3 and Ga_2O_3 precursor oxides, and alternatives with a lower cost are desired.

In a very recent work,¹⁹ Randall et al. have studied the existence of a MPB for the system $(1-x)\text{Bi}(\text{Mg}_{1/2}\text{Ti}_{1/2})\text{O}_3$ – $(x)\text{PbTiO}_3$, and stated its presence as having a composition range between $x = 0.36$ and 0.38 . For processing, they used a two-step route for the synthesis of the ceramic powders. MgTiO_3 was first formed by solid-state reaction of MgCO_3 and TiO_2 at 1400°C , and then reacted with Bi_2O_3 , PbCO_3 and additional TiO_2 for obtaining $\text{Bi}(\text{Mg}_{1/2}\text{Ti}_{1/2})\text{O}_3$ – PbTiO_3 in a second step. Sintering was also accomplished in two steps, where successive conventional and pressure assisted thermal treatments were applied for obtaining the ceramics. These presented a core-shell domain microstructure within a grain that suggested the presence of a

$\text{Bi}(\text{Mg}_{1/2}\text{Ti}_{1/2})\text{O}_3$ rich core surrounded by a PbTiO_3 rich shell. It was believed that this microstructure limited the piezoelectric activity of the ceramics. In the same work, they also established the ferro-paraelectric phase transition to be at 478°C (slightly higher than that for MPB $(1-x)\text{BiScO}_3$ – $(x)\text{PbTiO}_3$). Maximum values of $d_{33} = 225 \text{ pC N}^{-1}$ were obtained, but the dependence of the piezoelectric properties on temperature was not studied.

We report here a study of the processing of this new system by using a simpler route. This consisted of synthesising the powders by a one step, direct solid-state reaction of the constituent oxides, and of sintering the ceramics also in a single step without using pressure. Besides characterising the dielectric properties as a function of temperature and frequency, we also studied for the first time the piezoelectric properties as a function of temperature, and therefore identified the depoling temperature and assessed the potential for high temperature applications.

2. Experimental procedure

$(1-x)\text{Bi}(\text{Mg}_{1/2}\text{Ti}_{1/2})\text{O}_3$ – $(x)\text{PbTiO}_3$ ceramic powders were synthesised by one step, direct solid-state reaction of the constituent oxides. PbO , TiO_2 , Bi_2O_3 and MgO were weighed out and mixed in water. After drying, the powder was calcined at 900°C for 2 h and subsequently ball-milled to a median particle size of $\approx 2 \mu\text{m}$, as determined by laser scattering (Malvern MasterSizer E, Malvern Instruments Ltd). A binder was added prior to spray drying and pellets were pressed uniaxially at 100 MPa to a green diameter of 18.5 mm . Sintering was carried out for 2 h at 1000 and 1100°C . Sintered ceramics presented values of density of $\sim 95\text{--}97\%$ of the theoretical ones, density being slightly higher for samples sintered at 1000°C than for those sintered at 1100°C . Experimental values were obtained by the Archimedes' method, while theoretical ones were obtained from the X-ray diffraction data.

Perovskite phase formation and second phases were determined by Bragg–Brentano X-ray diffraction (XRD) with a Siemens D500 powder diffractometer, $\text{Cu K}\alpha$ radiation (1.5418 \AA) using a scan rate of $1 \times 10^{-2} 2\theta \text{ s}^{-1}$ in the $20\text{--}50^\circ 2\theta$ range. Slow scans at $2 \times 10^{-3} 2\theta \text{ s}^{-1}$ were accomplished across the split (200) diffraction peak of the prototype cubic perovskite in order to study its distortion and to assess the existence of a MPB. Split peaks were deconvoluted with the profile tool of the Siemens DIFFRAC AT V3.3 by using pseudovoigt functions.²⁰

Samples for microstructural characterisation were prepared by polishing one surface of the as sintered ceramics with Al_2O_3 suspension up to $0.1 \mu\text{m}$, and by thermal etching at 900°C (for 15 min) and quenching for revealing the grain structure. Optical microscopy (OM) and scanning electron microscopy (SEM) after carbon coating were used for characterising the samples. SEM was carried out with a 960 Zeiss SEM apparatus at 20 kV accelerating voltage. X-ray energy-dispersive spectrometry (EDXS, Link Isis, Oxford) was also accomplished in the SEM for compositional analysis.

The temperature dependence of the dielectric permittivity and losses was measured by impedance spectroscopy with a HP4194A analyser at several frequencies between 1 kHz and 1 MHz , and up to 900°C . Measurements were accomplished on

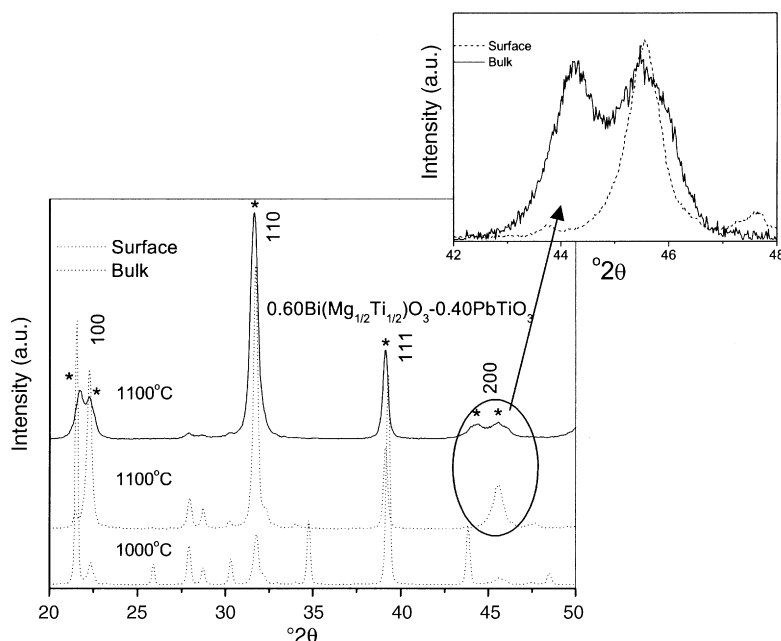


Fig. 1. XRD patterns for $0.60\text{Bi}(\text{Mg}_{1/2}\text{Ti}_{1/2})\text{O}_3\text{-}0.40\text{PbTiO}_3$ ceramics sintered at 1000 and 1100 °C perovskite peaks. Miller indexes referred to the parent cubic phase. Inset: slow scan XRD patterns across the split (200) diffraction peak of the prototype cubic perovskite for the ceramic sintered at 1100 °C.

ceramic discs after removing at least 0.4 mm from each side, and on which Pt electrodes were painted and sintered at 700 °C. The experimental set-up for the temperature control is described elsewhere.²¹ 1 °C min⁻¹ heating and cooling rates were used.

Analogous discs, though with Ag electrodes deposited by screen printing, were used for poling. Electric fields up to 5 kV mm⁻¹ were applied for 5 min at 100 °C. These field and time conditions were the highest that could be applied without causing dielectric breakdown. Piezoelectric d_{33} coefficients were measured by the direct piezoelectric effect with a Berlincourt-type meter at 100 Hz. Piezoelectric d_{31} coefficients as a function of temperature were obtained by analysis of the piezoelectric radial resonances of the discs by an automatic iterative method described elsewhere.²² This method has been widely used in the characterisation of an ample number of ceramics, such as modified lead titanate,⁹ commercial soft PZT²³ and BLSF.¹³

3. Results and discussion

Fig. 1 shows the X-ray diffraction patterns for $0.60\text{Bi}(\text{Mg}_{1/2}\text{Ti}_{1/2})\text{O}_3\text{-}0.40\text{PbTiO}_3$ ceramics sintered at 1000 and 1100 °C. The dotted lines are the patterns for the ceramics before any lapping, i.e. of their surface, while the solid line is the pattern for the ceramic sintered at 1100 °C after lapping, i.e. after the surface has been removed and so, of the bulk. Results indicate that a second phase has been formed at the surface, its amount being higher for the ceramics sintered at 1000 °C than for those sintered at 1100 °C. They also showed that the bulk is virtually free of these second phases and that a perovskite phase as reported in ref. ¹⁹ has formed. The inset in Fig. 1 shows the slow scan patterns across the split (200) diffraction peak of the prototype cubic perovskite for both

the surface and bulk of the ceramic sintered at 1100 °C. This peak was not split for the surface but it was split into three peaks for the bulk, which indicated the presence of a gradient of perovskite distortion within the ceramic. The perovskite at the surface, in coexistence with the second phase, seems to be rhombohedral, i.e. shifted towards $\text{Bi}(\text{Mg}_{1/2}\text{Ti}_{1/2})\text{O}_3$, while the perovskite in the bulk, free of second phases, presents coexistence of rhombohedral and tetragonal phases as expected according to ref. ¹⁹. Analogous results were obtained for the other two compositions.

EDXS measurements were carried out on samples before and after lapping for studying the composition of the second phases at the surface. It was found that the surface was Bi-rich and Mg-deficient as compared with the bulk, the difference being higher for samples sintered at 1000 °C than for those sintered at 1100 °C, i.e. directly related to the amount of second phases observed by XRD. Significant differences between the composition of the bulk of samples sintered at the two temperatures were not found.

Fig. 2a shows the slow scan pattern across the split (200) diffraction peak of the prototype cubic perovskite for a $0.60\text{Bi}(\text{Mg}_{1/2}\text{Ti}_{1/2})\text{O}_3\text{-}0.40\text{PbTiO}_3$ ceramic sintered at 1100 °C (bulk), and the fit of the pattern to three peaks with pseudo-Voigt type functions. According to ref. ¹⁹ the peak at 45.5°2θ is the (200) of the rhombohedral structure, and the peaks at 44.5 and 46°2θ are the (002) and (200) of the tetragonal phase, respectively. This was observed for the three compositions and two sintering temperatures and confirms the coexistence of rhombohedral and tetragonal phases, and thus the existence of a MPB in the $(1-x)\text{Bi}(\text{Mg}_{1/2}\text{Ti}_{1/2})\text{O}_3\text{-}(x)\text{PbTiO}_3$ system around the compositions studied. The ratio between the intensity of the rhombohedral (200) diffraction peak and the tetragonal (002)/(200) ones, $r = I_{\text{R-(200)}}/(I_{\text{T-(002)}} + I_{\text{T-(200)}})$, obtained from

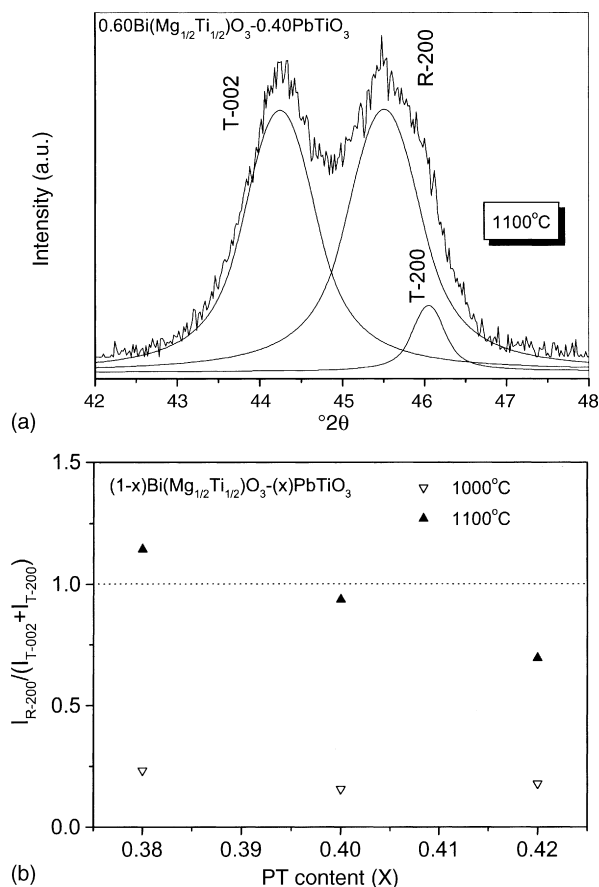


Fig. 2. (a) Slow scan XRD pattern across the split (200) diffraction peak of the prototype cubic perovskite for a $0.60\text{Bi}(\text{Mg}_{1/2}\text{Ti}_{1/2})\text{O}_3-0.40\text{PbTiO}_3$ ceramic sintered at 1100°C (bulk). The fit to three pseudo-Voigt type functions is also given; (b) ratio between the intensity of the rhombohedral (200) diffraction peak and the tetragonal (002)/(200) ones, obtained from the fits.

the fits is given in Fig. 2b as a function of composition and sintering temperature. This ratio is a measure of the relative percentages of rhombohedral and tetragonal phases. The ratio decreased when the PT content increased as expected. It also significantly increased with the sintering temperature, which seems to suggest problems in the incorporation of $\text{Bi}(\text{Mg}_{1/2}\text{Ti}_{1/2})\text{O}_3$ into the structure, this being easier the higher the temperature. This is likely to be associated with the appearance of Bi-rich second phases at the surface.

Fig. 3 shows OM images of polished surfaces for all $(1-x)\text{Bi}(\text{Mg}_{1/2}\text{Ti}_{1/2})\text{O}_3-(x)\text{PbTiO}_3$ ceramics. It was observed that porosity increases when the content of PbTiO_3 decreases, and when the sintering temperature increases. Some degree of pull-out occurred during polishing that corresponds to the largest dark features, marked with asterisks in the figure. It was more significant for the ceramics sintered at 1100°C than for those sintered at 1000°C , and is thought to be related with second phases as will be shown in Fig. 4. This shows SEM images of the same surfaces after thermal etching for revealing the grain structure. The ceramics mainly consist of equiaxed grains in which clusters of platelet-like grains are embedded. Point EDXS showed that the platelet-like grains are Bi-rich and Mg-deficient as compared with the equiaxed grains. This suggests that the

platelet-like grains are the second phases observed at the surface by XRD while the equiaxed grains are the perovskite phase. The platelets have a typical Aurivillius-type structure grain morphology, which is also consistent with a composition rich in Bi.²⁴ The platelet clusters are pulled out during polishing, giving rise to the large cavities observed by OM. The number of these clusters increased when the PT content decreased, and their size increased with increasing sintering temperature. The size of the perovskite grains did not change with composition but increased with the sintering temperature as can be seen in the figure.

This structural and microstructural characterisation indicates that there is an issue with the complete incorporation of $\text{Bi}(\text{Mg}_{1/2}\text{Ti}_{1/2})\text{O}_3$ into the structure, which is associated with the segregation of Bi at the surface and the formation of bismuth layered perovskite structure second phases. Results also showed that incorporation is improved by increasing the temperature up to 1100°C . The difficulty in the processing of the $(1-x)\text{Bi}(\text{Mg}_{1/2}\text{Ti}_{1/2})\text{O}_3-(x)\text{PbTiO}_3$ solid solution was expected from the tolerance factor of $\text{Bi}(\text{Mg}_{1/2}\text{Ti}_{1/2})\text{O}_3$, t , which is given by the equation:

$$t = \frac{R_A + R_O}{\sqrt{2}(R_B + R_O)} \quad (1)$$

where R_A and R_B are the ionic radius of the ions occupying the A, B positions, respectively, and R_O is the ionic radius of oxygen. The relatively small ionic radius of Bi^{3+} ($R_{\text{Bi}} = 1.03 \text{ \AA}$) in the A position (coordination 12) and the large ionic radius, mainly of Mg^{2+} ($R_{\text{Mg}} = 0.72 \text{ \AA}$), in the B position (coordination 6), both referred to the general ABO_3 perovskite, result in a small tolerance factor ($t = 0.862$ for $x = 0.40$). Perovskites with such tolerance factors are known to be difficult to synthesise and second phases often appear.¹⁴ For instance, the BiScO_3 -rich edge of the BiScO_3 - PbTiO_3 solid solution, with tolerance factors as low as $t = 0.78$ for BiScO_3 , can only be synthesised with high-pressure assisted methods.²⁵ This is possibly why, in their recent work, Randall et al. used a second sintering treatment under pressure.¹⁹

A second issue is probably PbO volatilisation at the surface, an effect that is more significant, the higher the sintering temperature. This is confirmed by the increase of porosity with temperature, and by the formation of a rhombohedral perovskite at the surface at 1100°C . Nevertheless, and though both effects have to be taken into account, basically single phase MPB perovskite materials have been obtained for the three compositions and two sintering temperatures after removing the surface, with only slight differences in the percentages of rhombohedral and tetragonal phases, without using pressure assisted techniques. Properties now presented correspond to such thinned ceramic samples.

Fig. 5 shows the temperature dependence of the dielectric permittivity and losses for the MPB $\text{Bi}(\text{Mg}_{1/2}\text{Ti}_{1/2})\text{O}_3$ - PbTiO_3 ceramics sintered at 1100°C . Similar results were obtained for the samples sintered at 1000°C . Fig. 5a compares the dielectric permittivity and losses on heating for the three compositions at 500 kHz. Two well-defined maxima with temperature were observed for all the ceramics. The anomalies were present both on heating and cooling, and showed hardly any dispersion

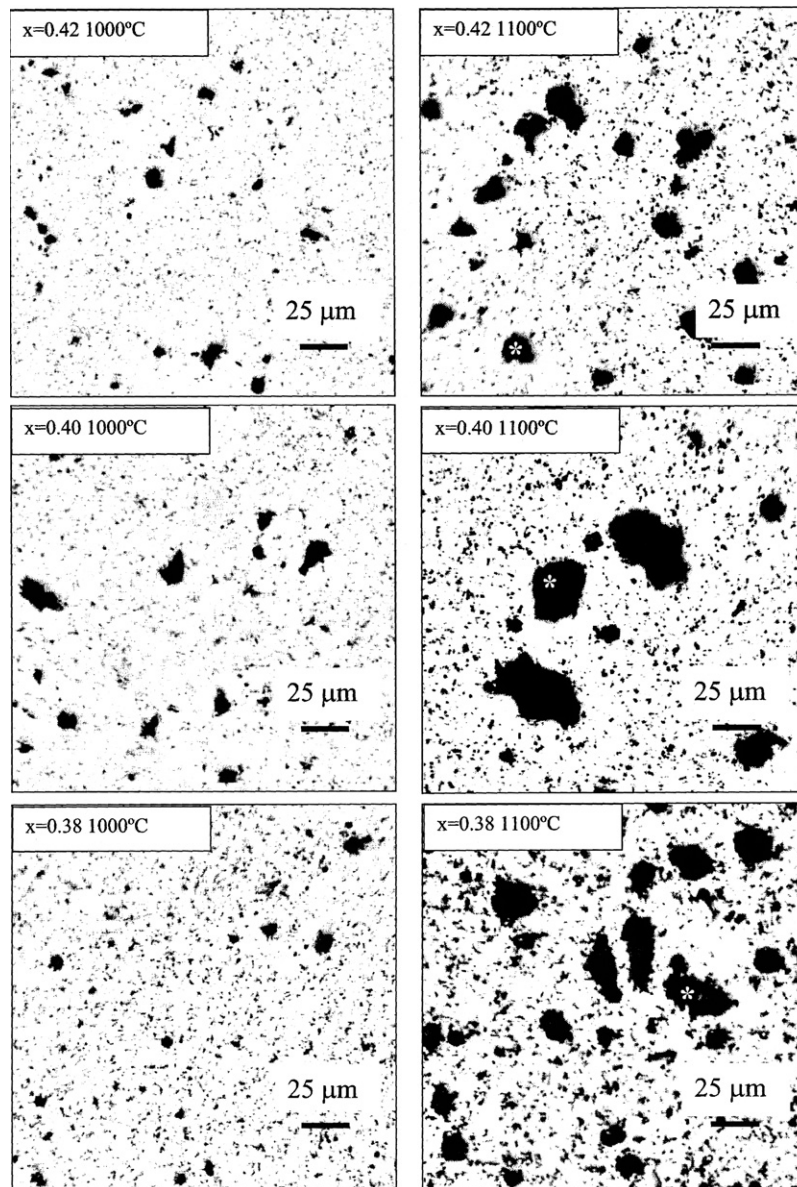


Fig. 3. Optical micrographs of the polished surfaces of $\text{Bi}(\text{Mg}_{1/2}\text{Ti}_{1/2})\text{O}_3\text{-PbTiO}_3$ sintered ceramics.

as it is illustrated in Fig. 5b and c for $0.58\text{Bi}(\text{Mg}_{1/2}\text{Ti}_{1/2})\text{O}_3\text{-}0.42\text{PbTiO}_3$. Therefore, both are most probably associated with phase transitions, the one at a higher temperature associated with the ferroelectric to paraelectric phase transition that is then located at $\sim 600^\circ\text{C}$. It must be noted that Randall et al.¹⁹ only observed this anomaly for rhombohedral compositions, and less well-defined, but not for MPB and tetragonal samples and did not associate it with the ferroelectric transition but to some unknown phenomena. However, we have observed it for all the MPB samples studied here involving a number of compositions and sintering temperatures. The core-shell grain structure observed in ref.¹⁹ could be behind this discrepancy. The broadening of the anomaly could be associated with residual gradients of composition, but mainly with the disorder that results from the simultaneous occupation of the A and B sites by two different cations. The anomaly at a lower temperature is located

at $\sim 350^\circ\text{C}$ and is most probably associated with a second phase transition. A similar anomaly has been observed for rhombohedral $(1-x)\text{BiScO}_3\text{-}x\text{PbTiO}_3$ single crystals with $x=0.55$ ²⁶ and 0.57 ,¹⁶ and attributed to a ferroelectric rhombohedral to ferroelectric tetragonal phase transition. Another possibility could be a ferroelectric to antiferroelectric phase transition similar to that reported for $(\text{Na}_{0.5}\text{Bi}_{0.5})\text{TiO}_3\text{-BaTiO}_3$.²⁷ Unfortunately ferroelectric hysteresis loops for our samples could not be traced at high temperature because of d.c. conduction. This conduction can be observed in the dielectric losses, and is responsible for the highly dispersive minimum at low temperatures. The d.c. conduction has been reported for $\text{BiScO}_3\text{-PbTiO}_3$, though the mechanism, either ionic or electronic, has not been stated.²⁸

Fig. 6 shows the room temperature piezoelectric coefficient d_{33} as a function of PT content and sintering temperature, after poling with 5 kV mm^{-1} . Ceramics sintered at 1000°C presented

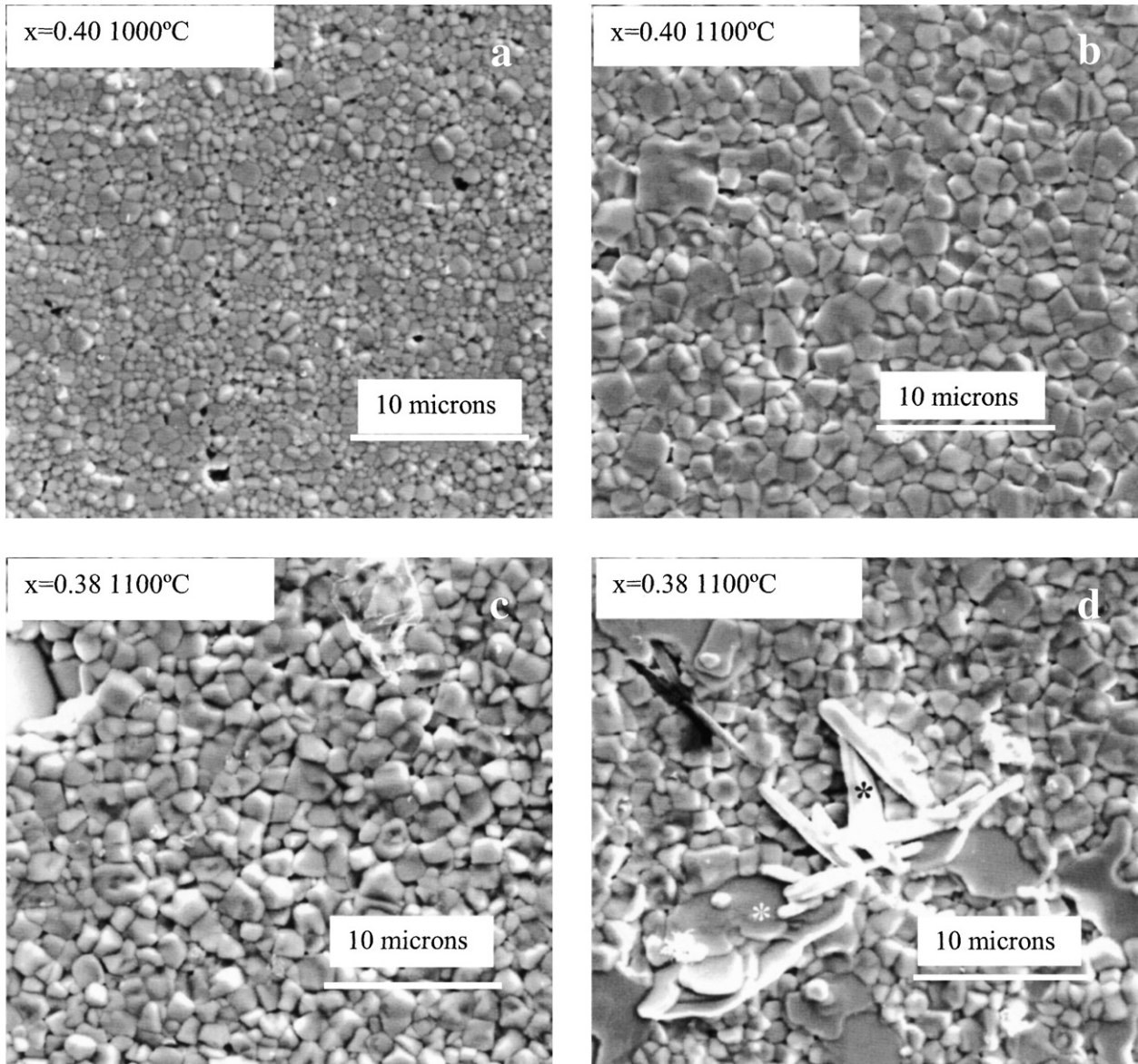


Fig. 4. SEM micrographs of polished and thermally etched surfaces of $\text{Bi}(\text{Mg}_{1/2}\text{Ti}_{1/2})\text{O}_3\text{-PbTiO}_3$ sintered ceramics.

d_{33} values significantly higher than those sintered at 1100°C . Those with $x=0.38$ could only withstand fields of 4 kV mm^{-1} and a $d_{33} = 126\text{ pC N}^{-1}$ was obtained. Ceramics with $x=0.40$ and 0.42 withstood fields of 5 kV mm^{-1} and coefficients of $d_{33} = 166$ and 157 pC N^{-1} were obtained, respectively. Ceramics sintered at 1100°C presented d_{33} values of $\sim 100\text{ pC N}^{-1}$ with little dependence of the PT content. 5 kV mm^{-1} was the highest field that could be applied at 100°C before electrical breakdown. This is most probably the reason why the highest coefficients here obtained are slightly below those of Randall et al.,¹⁹ where poling fields as high as 6.5 kV mm^{-1} could be applied. Values of $d_{33} \geq 200\text{ pC N}^{-1}$ were reported in ref.¹⁹. The d.c. conductivity then prevents full saturation to be reached for our ceramics. This conductivity could originate from minor second phases at the grain boundaries or point defects in the structure associated with the issue of $\text{Bi}(\text{Mg}_{1/2}\text{Ti}_{1/2})\text{O}_3$ incorporation, or the volatilisation of PbO . The piezoelectric coefficients being higher for

ceramics sintered at 1000°C than for those sintered at 1100°C can be explained by the combination of microstructural factors, most probably the increase in porosity, and the lack of saturation. Small differences in porosity do not result in large differences in remnant polarisation and piezoelectric coefficients in saturation, but can cause large differences in piezoelectric coefficients when non-saturating fields are used, as is the case here.

In addition to measurements at room temperature, the piezoelectric activity was also studied as a function of temperature and is reported here for the first time. Fig. 7 shows the temperature dependence of the piezoelectric coefficient d_{31} for all the MPB $\text{Bi}(\text{Mg}_{1/2}\text{Ti}_{1/2})\text{O}_3\text{-PbTiO}_3$ ceramics, expressed as relative changes from the room temperature values as defined in Eq. (2):

$$\Delta d_{31}(T) = \frac{d_{31}(T) - d_{31}(RT)}{d_{31}(RT)} \times 100, \quad (2)$$

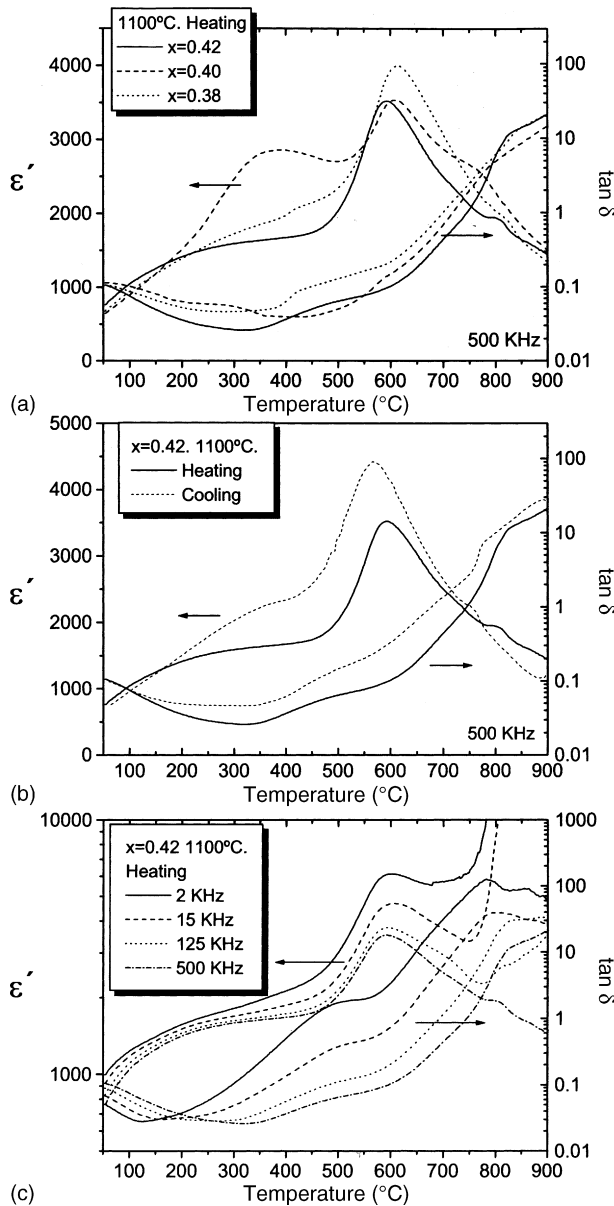


Fig. 5. (a) Dielectric permittivity and losses at 500 kHz as a function of temperature for $\text{Bi}(\text{Mg}_{1/2}\text{Ti}_{1/2})\text{O}_3\text{-PbTiO}_3$ ceramics sintered at 1100 °C on heating; (b) same magnitudes for ceramics with $x=0.42$ on both heating and cooling; (c) same magnitudes for ceramics with $x=0.42$ at four different frequencies on heating.

where $d_{31}(\text{RT})$ is the value at room temperature. d_{31} coefficients were obtained by analysis of piezoelectric radial resonances of discs. d_{31} initially increased for all ceramics up to values that can be as high as twice the RT value at temperatures between 150 and 250 °C, above which it decreased until complete depoling at temperatures between 200 and 300 °C, mainly depending on the sintering temperature. Ceramics sintered at 1000 °C still maintained a significant piezoelectric activity at 300 °C with a relative decrease of coefficients smaller than 40%, while those sintered at 1100 °C were fully depoled at 250 °C. Maxima of piezoelectric coefficients with temperature have been described for other perovskite MPB systems such as $\text{Pb}(\text{Mg}_{1/3}\text{Nb}_{2/3})\text{O}_3\text{-PbTiO}_3$,²⁹ $\text{Pb}(\text{Zn}_{1/3}\text{Nb}_{2/3})\text{O}_3\text{-PbTiO}_3$ ³⁰ and $\text{BiScO}_3\text{-PbTiO}_3$ ²⁶

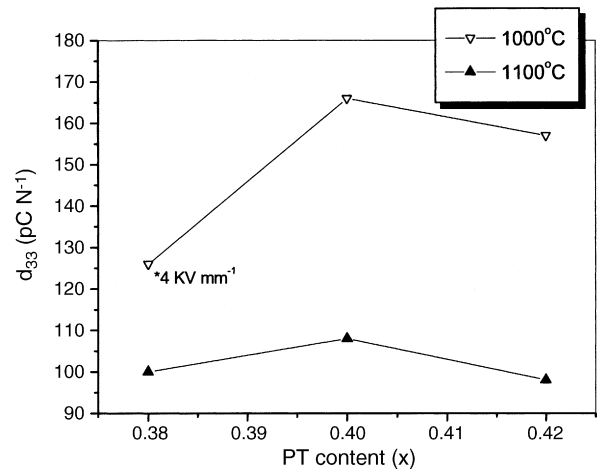


Fig. 6. RT piezoelectric coefficient d_{33} as a function of PT content (Poling field: 5 kV mm⁻¹ except 4 kV mm⁻¹).

and associated with the rhombohedral to tetragonal phase transition, which must be also the case for the system studied here. This transition has also been proposed to be the origin of depoling for $\text{BiScO}_3\text{-PbTiO}_3$. The dependence of the depoling temperature on sintering temperature here observed seems to support depoling being associated with the transition. Zhang et al. have shown that an increase of PbTiO_3 (tetragonal) content in the $\text{BiScO}_3\text{-PbTiO}_3$ solid solution from 0.55²⁶ to 0.57¹⁶ produces an increase of the rhombohedral to tetragonal phase transition temperature from 301 to 349 °C. For the ceramics here studied, those sintered at 1000 °C showed incomplete $\text{Bi}(\text{Mg}_{1/2}\text{Ti}_{1/2})\text{O}_3$ incorporation as compared with the samples sintered at 1100 °C, and so are effectively shifted towards the tetragonal PT edge. It must be said that the rhombohedral to tetragonal phase transition does not cause depoling for $\text{Pb}(\text{Mg}_{1/3}\text{Nb}_{2/3})\text{O}_3\text{-PbTiO}_3$, so some role of other phenomena, such as d.c. conduction, cannot be ruled out.

It is worth noting that the MPB $\text{Bi}(\text{Mg}_{1/2}\text{Ti}_{1/2})\text{O}_3\text{PbTiO}_3$ ceramics sintered at 1000 °C present piezoelectric coefficients significantly higher than lead metaniobate and can

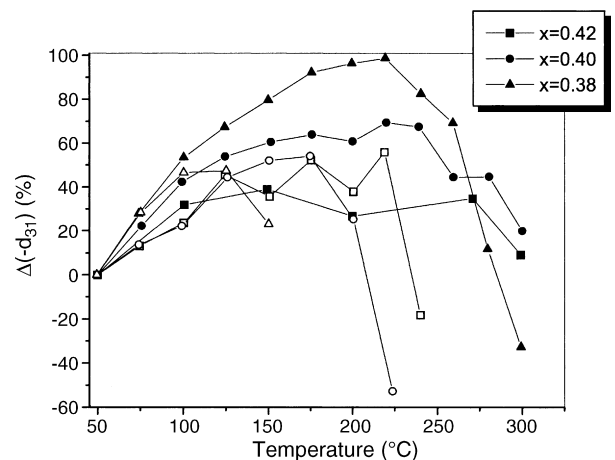


Fig. 7. Temperature dependence of the relative (to the RT values) piezoelectric coefficient d_{31} (closed symbols: sintered at 1000 °C; open symbols: sintered at 1100 °C).

also maintain the piezoelectricity up to a temperature of 300 °C. Also, depoling occurs well below the Curie temperature at ~600 °C, and so it could be possible to increase the temperature range of piezoelectric activity. However, a number of issues need to be addressed and solved, such as d.c. conductivity that limits the poling fields and prevents saturation to be reached, and the mechanisms of depoling at 300 °C.

4. Conclusions

MPB $\text{Bi}(\text{Mg}_{1/2}\text{Ti}_{1/2})\text{O}_3\text{-PbTiO}_3$ has been successfully processed by conventional sintering (without pressure assisted techniques) from powders synthesised by one step, direct solid-state reaction of the constituent oxides. $\text{Bi}(\text{Mg}_{1/2}\text{Ti}_{1/2})\text{O}_3$ incorporation is an issue, which is associated with the presence of Aurivillius type phases at the surface, and it improves by increasing the sintering temperature from 1000 to 1100 °C. PbO volatilisation is a second issue, and a rhombohedral $\text{Bi}(\text{Mg}_{1/2}\text{Ti}_{1/2})\text{O}_3$ rich perovskite is formed at 1100 °C, also at the surface. Nevertheless, basically single phase MPB $\text{Bi}(\text{Mg}_{1/2}\text{Ti}_{1/2})\text{O}_3\text{-PbTiO}_3$ is formed in the bulk, with slight differences between the percentages of rhombohedral and tetragonal phases, depending on sintering temperature. This parameter also affects porosity and grain size that increase with the temperature.

Dielectric permittivity presented two maxima with temperature at 300–400 °C and ~600 °C. The anomalies were observed both on heating and cooling and showed hardly any dispersion. Therefore, both are most probably associated with phase transitions, the one at a higher temperature associated with the ferroelectric to paraelectric phase transition, and the one at a lower temperature with the rhombohedral to tetragonal phase transition. This is a discrepancy from previous results by Randall et al., who reported the Curie temperature to be at a significantly lower temperature.

Saturation could not be attained during poling because of d.c. conductivity, though piezoelectric coefficients approaching those previously reported by Randall et al. were achieved after poling with 5 kV mm^{-1} at 100 °C for ceramics sintered at 1000 °C. These ceramics maintained piezoelectricity up to 300 °C, and depoling occurred above this temperature, most probably associated with the rhombohedral to tetragonal phase transition. This system is then an alternative to commercial ceramics operating at the intermediate range of temperatures between 200 and 300 °C, and has the potential to reach higher temperatures because of its Curie temperature at 600 °C.

Acknowledgments

This work has been funded by the European Commission (PIRAMID Growth Project, ref. G5RD-CT-2001-00456), the Spanish MEC (Projects MAT2001-4819-E, MAT2002-00463 and Ramón y Cajal Programme) and the Spanish CAM (Project 07N/0076/2002).

References

1. Damjanovic, D., Materials for high temperature piezoelectrics transducers. *Curr. Opin. Solid State Mater. Sci.*, 1998, **3**, 469–473.
2. Shrout, T. R., Eitel, R. E. and Randall, C. A., *Piezoelectric Materials in Devices*. Ed. N. Setter, 2002, pp. 413–432.
3. Ferroperm Full Catalogue in <http://www.ferroperm-piezo.com>.
4. Yasuda, N., Ohwa, H., Kune, M. and Yamashita, Y., Crystal growth and electrical properties of lead indium niobate-lead titanate binary single crystal. *J. Cryst. Growth*, 2001, **229**, 299–304.
5. Zhang, S. J., Rhee, S., Randall, C. A. and Shrout, T. R., Dielectric and piezoelectric properties of high Curie temperature single crystals in the $\text{Pb}(\text{Yb}_{1/2}\text{Nb}_{1/2})\text{O}_3\text{-xPbTiO}_3$ solid solution series. *Jpn. J. Appl. Phys.*, 2002, **41**, 722–726.
6. Zhang, S. J., Laurent, L., Rhee, S., Randall, C. A. and Shrout, T. R., Shear-mode piezoelectric properties of $\text{Pb}(\text{Yb}_{1/2}\text{Nb}_{1/2})\text{O}_3\text{-PbTiO}_3$ single crystals. *Appl. Phys. Lett.*, 2002, **81**, 892–894.
7. Damjanovic, D., Gururaja, T. R. and Cross, L. E., Anisotropy in piezoelectric properties of modified lead titanate ceramics. *Am. Ceram. Soc. Bull.*, 1987, **66**(4), 699–703.
8. Ricote, J., Alemany, C. and Pardo, L., Microstructural effects on dielectric and piezoelectric behaviour of calcium-modified lead titanate ceramics. *J. Mater. Res.*, 1995, **10**(12), 3194–3203.
9. Ricote, J., Alemany, C., Pardo, L. and Millar, C. E., Microstructure-properties relationships in samarium modified lead titanate piezoceramics. Part II. Dielectric, piezoelectric and mechanical properties. *Acta Mater.*, 1996, **44**(3), 1169–1179.
10. Schulz, M. J., Sundaresan, M. J., McMichael, J., Clayton, D., Sadler, R. and Nagel, B., Piezoelectric materials at elevated temperature. *J. Intel. Mat. Syst. Str.*, 2003, **14**(11), 693–705.
11. Aurivillius, B., Mixed bismuth oxides with layer lattices: I, structure type of $\text{CaCb}_2\text{Bi}_2\text{O}_9$. *Arkiv. Kemi.*, 1949, **1**(54), 463–480.
12. Aurivillius, B., II, structure type of $\text{Bi}_4\text{Ti}_3\text{O}_{12}$. *Arkiv. Kemi.*, 1949, **1**(58), 499–512.
13. Moure, A., Alemany, C. and Pardo, L., Temperature dependence of piezoelectric, elastic and dielectric coefficients at radial resonance of piezoceramics with an aurivillius-type structure. *IEEE T. Ultrasonic Ferr.*, 2005, **52**(4), 570–577.
14. Eitel, R. E., Randall, C. A., Shrout, T. R., Rehrig, P. W., Hackenberger, W. and Park, S. E., New high temperature morphotropic phase boundary piezoelectrics based on $\text{Bi}(\text{Me})\text{O}_3\text{-PbTiO}_3$ ceramics. *Jpn. J. Appl. Phys.*, 2001, **40**, 5999–6002.
15. Eitel, R. E., Randall, C. A., Shrout, T. R. and Park, S. E., Preparation and characterization of high temperature perovskite ferroelectrics in the solid-solution $(1-x)\text{BiScO}_3\text{-xPbTiO}_3$. *Jpn. J. Appl. Phys.*, 2002, **41**, 2099–2104.
16. Zhang, S., Randall, C. A. and Shrout, T. R., High Curie temperature piezocrystals in the $\text{BiScO}_3\text{-PbTiO}_3$ perovskite system. *Appl. Phys. Lett.*, 2003, **83**(15), 3150–3152.
17. Cheng, J., Eitel, R. E., Li, N. and Cross, L. E., Structural and electrical properties of $(1-x)\text{Bi}(\text{Ga}_{1/4}\text{Sc}_{3/4})\text{O}_3\text{-xPbTiO}_3$ piezoelectric ceramics. *J. Appl. Phys.*, 2003, **94**(1), 605–609.
18. Cheng, J. and Cross, L. E., Effects of La substituent on ferroelectric rhombohedral/tetragonal morphotropic phase boundary in $(1-x)(\text{Bi},\text{La})(\text{Ga}_{0.05}\text{Fe}_{0.95})\text{O}_3\text{-xPbTiO}_3$ piezoelectric ceramics. *J. Appl. Phys.*, 2003, **94**(8), 5188–5192.
19. Randall, C. A., Eitel, R. E., Jones, B., Shrout, T. R., Woodward, D. I. and Reaney, I. M., Investigation of a high T-c piezoelectric system: $(1-x)\text{Bi}(\text{Mg}_{1/2}\text{Ti}_{1/2})\text{O}_3\text{-(x)PbTiO}_3$. *J. Appl. Phys.*, 2004, **95**(7), 3633–3639.
20. Profile user's guide (VI.4) Diffract-AT V3 software package (SOCABIM, France) for DACO-PM SIEMENS D-500 diffractometer controller.
21. Durán-Martín, P. Propiedades ferroeléctricas de materiales cerámicos con estructura tipo Aurivillius de composiciones basadas en $\text{SrBi}_2\text{Nb}_2\text{O}_9$, Ph.D. thesis, Universidad Autónoma de Madrid, 1997.
22. Alemany, C., Gonzalez, A. M., Pardo, L., Jimenez, B., Carmona, F. and Mendiola, J., Automatic determination of complex constants of piezoelec-

- tric materials in the radial mode. *J. Phys. D: Appl. Phys.*, 1995, **28**, 945–956.
23. Alguero, M., Alemany, C., Pardo, L. and Gonzalez, A. M., Method for obtaining the full set of linear electric, mechanical, and electromechanical coefficients and all related losses of a piezoelectric ceramic. *J. Am. Ceram. Soc.*, 2004, **87**(2), 209–215.
 24. Holmes, M., Newnham, R. E., and Cross, L.E., Grain-oriented ferroelectric ceramics. *Am. Ceram. Soc. Bull.*, 1979, **58**, 872–872.
 25. Inaguma, Y., Miyaguchi, A., Yoshida, M. and Katsumata, T., High-pressure synthesis and ferroelectric properties in perovskite-type $\text{BiScO}_3\text{-PbTiO}_3$ solid solution. *J. Appl. Phys.*, 2004, **95**, 231–235.
 26. Zhang, S., Randall, C. A. and Shrout, T. R., Electromechanical properties in rhombohedral $\text{BiScO}_3\text{PbTiO}_3$ single crystals as a function of temperature. *Jpn. J. Appl. Phys.*, 2003, **42**, L1152–L1154.
 27. Li, Y., Chen, W., Zhou, J., Xu, Q., Sun, H. and Xu, R., Dielectric and piezoelectric properties of lead-free $(\text{Na}_{0.5}\text{Bi}_{0.5})\text{TiO}_3\text{-NaNbO}_3$ ceramics. *Mater. Sci. Eng. B*, 2004, **112**, 5–9.
 28. Porokhonsky, V., Kamba, S., Pashkin, A., Savinov, M., Eitel, R. E. and Randall, C. A., Broadband dielectric spectroscopy of $(1-x)\text{BiScO}_3\text{-xPbTiO}_3$ piezoelectrics. *Appl. Phys. Lett.*, 2003, **83**(8), 1605–1607.
 29. Wang, P. C., Pan, X. M., Li, D. L., Song, Y. W., Lao, H. S. and Yin, Z. W., Temperature dependence of piezoelectric properties of $0.67\text{Pb}(\text{Mg}_{1/3}\text{Nb}_{2/3})\text{O}_3\text{-}0.33\text{PbTiO}_3$ single crystals. *J. Mater. Res.*, 2003, **18**(2), 537–541.
 30. Kuwata, J., Uchino, K. and Nomura, S., Dielectric and piezoelectric properties of $0.91\text{Pb}(\text{Zn}_{1/3}\text{Nb}_{2/3})\text{O}_3\text{-}0.09\text{PbTiO}_3$ single crystals. *Jpn. J. Appl. Phys.*, 1982, **21**, 1298–1302.